NASA TECHNICAL NOTE

NASA TN D-6005

SPECTROSCOPIC ANALYSIS OF ELECTRON-BEAM-INDUCED FLUORESCENCE IN HYPERSONIC HELIUM FLOW

by Mervin E. Hillard, Jr., Stewart L. Ocheltree, and Richard W. Storey

Langley Research Center
Hampton, Va. 23365

NATIONAL AERONAUTICS AND SPACE ADMINISTRATION • WASHINGTON, D. C. • OCTOBER 1970

1. Report No.	2. Government Accession No.	3. Recipient's Catalog No.
NASA TN D-6005		

4. Title and Subtitle

SPECTROSCOPIC ANALYSIS OF ELECTRON-BEAM-INDUCED FLUORESCENCE IN HYPERSONIC HELIUM FLOW

5. Report Date: October 1970

6. Performing Organization Code

7. Author(s)

Mervin E. Hillard, Jr., Stewart L. Ocheltree, and Richard W. Storey

8. Performing Organization Report No.: L-7146

10. Work Unit No.: 129-01-22-12

9. Performing Organization Name and Address

NASA Langley Research Center
Hampton, Va. 23365

11. Contract or Grant No.

13. Type of Report and Period Covered: Technical Note

12. Sponsoring Agency Name and Address

National Aeronautics and Space Administration
Washington, D.C. 20546

14. Sponsoring Agency Code

15. Supplementary Notes

16. Abstract

The ability to visualize low-density hypersonic helium flow has been substantially improved through the use of a high-energy (26-keV) electron beam in the Langley 22-inch helium tunnel at a Mach number of about 20. It has been found that the electron beam efficiently excites the test gas to produce visible fluorescence throughout the flow field with a brightness which is dependent upon the local gas density.

The present investigation involved the spectroscopic analysis of the electron-beam-induced fluorescence. It was conducted in order to better understand the excitation and emission mechanisms involved and to use this knowledge to improve the visualization technique further. Spectrograms of the fluorescence, both in the free-stream and model flow fields, have been made; and the major radiating species have been identified as atomic helium, molecular helium, and the molecular nitrogen ion. The molecular nitrogen ion was found to be the emitter whose fluorescence enhanced the shock structure. Based on the results of this work, areas for further work have been identified.

17. Key Words (Suggested by Author(s))

Spectroscopic analysis
Electron-beam-induced fluorescence

18. Distribution Statement

Unclassified – Unlimited

19. Security Classif. (of this report)	20. Security Classif. (of this page)	21. No. of Pages	22. Price*
Unclassified	Unclassified	21	$3.00

*For sale by the Clearinghouse for Federal Scientific and Technical Information
Springfield, Virginia 22151

SPECTROSCOPIC ANALYSIS OF ELECTRON-BEAM-INDUCED FLUORESCENCE IN HYPERSONIC HELIUM FLOW

By Mervin E. Hillard, Jr., Stewart L. Ocheltree,
and Richard W. Storey
Langley Research Center

SUMMARY

The ability to visualize low-density hypersonic helium flow has been substantially improved through the use of a high-energy (26-keV) electron beam in the Langley 22-inch helium tunnel at a Mach number of about 20. It has been found that the electron beam efficiently excites the test gas to produce visible fluorescence throughout the flow field with a brightness which is dependent upon the local gas density.

The present investigation involved the spectroscopic analysis of the electron-beam-induced fluorescence. It was conducted in order to better understand the excitation and emission mechanisms involved and to use this knowledge to improve the visualization technique further. Spectrograms of the fluorescence, both in the free-stream and model flow fields, have been made; and the major radiating species have been identified as atomic helium, molecular helium, and the molecular nitrogen ion. The molecular nitrogen ion was found to be the emitter whose fluorescence enhanced the shock structure. Based on the results of this work, areas for further work have been identified.

INTRODUCTION

In hypersonic wind tunnels, the ability to visualize flow features about models by using conventional schlieren and shadowgraph techniques is severely limited by the low gas densities encountered in the test section. Frequently the performance of these techniques is degraded to the point where only the bow shock wave can be observed. This problem is compounded in helium wind tunnels because helium has a low refractive index which further reduces the sensitivity of optical flow-visualization techniques. One of the most promising methods suggested to improve this situation has been the use of an electrical discharge or electron beam to excite the gas upstream of a model being tested. (See refs. 1 to 6.) Under favorable gas-flow conditions, the resulting density-dependent fluorescence has sufficient brightness and persistence to envelop the model, be photographed, and thereby reveal the detailed flow structure throughout the model flow field. This phenomenon has been observed in the laboratory to be particularly effective in static tests where a small quantity of a secondary gas mixed with helium often results, upon

excitation, in enhancing part of the spectrum of the secondary gas. (See ref. 7.) Most of this work in helium has been done within the past decade; Niles and Robertson (ref. 8) investigated the time delay of afterglow emission in a dc-pulsed helium discharge; and Collins and Robertson (ref. 9) used a flowing system activated by a microwave discharge to investigate the excitation processes involved. Some variations of these methods are reported in references 10 to 17.

Recently, the electron-beam-excitation technique has been very successfully employed to improve the flow-visualization capability in the Langley 22-inch helium tunnel (ref. 18) where a 26-keV electron beam was used to excite Mach 20 helium-gas flow with a nominal static temperature of 2.5° K and number density of 6×10^{23} per m^3. The results of these early tests indicated the need to identify the physical mechanisms responsible for the extraordinarily bright and persistent fluorescence observed in this low-temperature, high-velocity helium flow. This knowledge was believed to be essential to further optimization of the electron-beam technique for low-density flow visualization and its extension to probeless gas-density and temperature measurements in helium flow.

The purpose of the present investigation was to first identify the primary radiating species by measuring the spectral content and spatial distribution of the fluorescence in Mach 20 helium flow and then to relate an explanation of these observations to future work. To accomplish the experimental phase of this investigation, two spectrographs were positioned to observe various regions of the test area: upstream and downstream of the electron beam, in the electron beam, and in the shock structure of a model. Spectrograms obtained were used to determine the spatial distribution of the fluorescence and to identify the primary radiators as the molecular nitrogen ion and atomic and molecular helium. A physical description of the excitation and emission mechanisms has been provided. Results from this study may be applied to future work in extending the use of the electron-beam technique in hypersonic helium flow.

SYMBOLS

$B^2\Sigma_u^+$	excited state of molecular nitrogen ion $\left(N_2^+\right)$
e	electron charge
f/	aperture ratio
h	Planck constant
3^1P, 3^3P, 2^1S, 2^3S	atomic states

$X^2\Sigma_g^+$ ground state of N_2^+

λ wavelength

ν wave frequency

$^3\Sigma_u^+$ metastable state of molecular helium

Superscripts:

m metastable state

* excited state

APPARATUS

The electron-gun system used in this investigation was developed at the Langley Research Center. A photograph of the gun with associated electronics is shown in figure 1. The gun consists of a directly heated tungsten-filament cathode, a reentrant cathode shield, and an anode drift tube. The tungsten filament and the cathode shield are operated at a negative 10 to negative 40 kilovolts potential with an additional negative bias applied to the shield for control of the beam current. The anode is held at ground potential; thus the high voltage hazard to operating personnel is eliminated.

The beam of electrons (0 to 1.5 mA) leaves the filament and passes through the 0.318-cm-diameter orifice in the cathode shield to the 1.9-cm-diameter opening in the anode entering the drift tube. The drift tube is 1.9 cm in diameter and 61 cm in length. The electrons are positioned magnetically in the center of the drift tube, focused by a magnetic lens, and then repositioned magnetically. This second positioning enables the beam to pass through the differential pumping section at the other end of the drift tube and emerge well collimated.

The differential pumping section, necessary to maintain a low pressure in the gun assembly, consists of two orifices 0.102 cm in diameter by 2.54 cm in length. The two orifices are separated by a chamber 2.54 cm in diameter and 2.54 cm in length, and this chamber is continually evacuated by a mechanical pump. By using this differential pumping section, a pressure of 2×10^{-5} to 2×10^{-4} mm Hg (2.7 mN/m^2 to 27 mN/m^2) can be maintained in the gun with pressure external to the gun as high as 10 mm Hg (1.3 kN/m^2).

For these tests the electron gun was placed on the top of the tunnel so that the beam entered the test section at the center line of the upstream window. The gun was mounted to the top of the tunnel by a vacuum-tight fitting which also electrically isolates the gun from the tunnel. The isolation of the gun permitted the tunnel test section to be used as a Faraday cage for beam-current collection.

Two spectrographs were used in these tests: a high-resolution spectrograph used to obtain spectra in the wavelength range from 3900 to 5050 Å (0.39 to 0.505 μm) and a low-resolution survey spectrograph which covered most of the visible region, 3500 to 6500 Å. The high-resolution spectrograph was used with a grating of 1200 grooves/mm blazed at a wavelength of 2000 Å and produced a dispersion of approximately 15 Å/mm. With this spectrograph, spectra were taken at slit widths of 100 and 300 μm with an exposure time approximately constant at 37 seconds and an effective aperture ratio of f/8.9. These spectra were recorded on ASA 3000 film. The survey spectrograph was used with a transmission grating of 600 grooves/mm and produces a dispersion of approximately 71 Å/mm. (See ref. 19.) The slit width was not calibrated on this instrument, but the widths used were comparable with those used on the high-resolution instrument, and the exposure time was 37 seconds also. The effective aperture ratio used was f/4, and the spectra were recorded on ASA 10 000 film. The optical arrangement applicable to both of these spectrographs is shown in figure 2. The basic setup consisted of the spectrograph and a collecting lens which imaged the source at the slit. A Dove prism was used in one test to rotate the image 90°.

The characteristics of the Langley 22-inch helium tunnel are presented in reference 20. The actual free-stream number densities used in the present study ranged from 6.4×10^{23} to 14.3×10^{23} per m^3, the static temperature from 2.2° to 2.5° K, and the gas composition from 40 to 400 parts per million of molecular nitrogen in helium.

EXPERIMENTAL PROCEDURE

Spectra were obtained from four regions representative of the fluorescence from the undisturbed flow (fig. 3) and from three regions representative of the fluorescence which exists when shock waves are present (fig. 4). These particular locations were selected because they usually appeared to possess distinctly different spectral characteristics. Table 1 contains the specific test conditions corresponding to each region.

The procedure for alining the spectrograph with the region of interest was basically the same for each region. The spectrograph was leveled and positioned perpendicular to the tunnel window. The optics were alined with the slit of the spectrograph; this alinement allowed any region of fluorescence to be observed by positioning the spectrograph table. Fine adjustments were made by placing a small tungsten lamp at the region of interest.

The initial tests were performed with the electron beam exciting the unperturbed flow. Regions 1, 3, and 4 in figure 3 were chosen to illustrate the fluorescence which exists upstream, downstream, and far downstream, respectively, from the region of direct excitation by the electron beam. For region 2, which includes both the region of direct-beam excitation and the region immediately downstream from the beam, the slit on the spectrograph was effectively rotated 90° by placing a Dove prism directly in front of the slit and thus making the slit appear parallel to the flow direction. This rotation was made to obtain a spectrum showing the spatial variation of the fluorescence in the flow direction. With this setup, the image of the electron beam was perpendicular to the slit, which allowed this image to be placed at one end of the slit such that the immediate downstream fluorescence illuminated the remaining slit length. Since the gas was flowing, the spatial variation of the fluorescence obtained in region 2 is equivalent to a time variation. This spectrum was obtained by using a magnification of 1 and a slit height of 1.8 cm to produce a total-time variation of 10 μsec at the free-stream velocity of 1.8 km/sec.

Next, the shock-wave fluorescence was investigated by using a 45° wedge model to create a bow and wake shock wave. Region 5 in figure 4 is representative of the fluorescence which is present upstream of the model, whereas regions 6 and 7 represent the shock-wave fluorescence explicitly. Since the shock position is known for this model, the spectrograph and collecting lens were positioned to image the bow shock wave, 2.54 cm downstream and 2.54 cm above the model at the slit of the spectrograph (region 6). Also a spectrum was taken farther downstream in the wake shock (region 7).

To qualitatively determine the effects of temperature on the free-stream gas fluorescence, a laboratory experiment was performed in a stationary gas mixture. The experimental setup and the gas number density were the same as those used in the dynamic test, but a static gas temperature of 300° K was used. Since the tunnel had a measured impurity range of 40 to 400 parts per million of nitrogen in helium, a helium test gas with 100 parts per million of nitrogen was used for the static test.

In an investigation of the effect of high-energy electrons scattering from the tunnel wall back into the flow, an electron collector placed at the bottom of the tunnel was utilized. The cylindrical collector was positioned such that the electron beam would be centered in it. This setup restricted the backscattering of primary electrons to less than 0.43 radian with respect to the primary beam.

RESULTS AND DISCUSSION

Analysis of spectrographic data obtained from the various observation regions in the wind tunnel indicated characteristic spectra of three radiating species: atomic helium (He), molecular helium (He_2), and the molecular nitrogen ion (N_2^+). The relative

emission intensities of these radiators were found to vary significantly and to change in order of brightness from region to region, as indicated in figures 3 and 4. In these figures the strongest radiator is listed first and the weakest, last. Figure 5 gives the energy-level diagram for these primary radiating species.

Unexpectedly strong radiation was observed from the molecular nitrogen ion at all observation points in these tests. For several decades, it has been known that upon excitation the radiation emitted by trace amounts of nitrogen in helium is enhanced. With the test conditions used in this experiment, the nitrogen radiation was greatly enhanced; therefore, the use of the electron-beam technique for flow visualization in hypersonic helium flow was improved. The nitrogen radiation observed was from the first negative system $\left(B^2\Sigma_u^+ - X^2\Sigma_g^+\right)$. (See fig. 5.) Figure 6 is the spectrum obtained in and near the electron beam (region 2 of fig. 3). This spectrum shows that atomic helium was the primary radiator in the electron beam and that molecular helium was the primary radiator near the beam. This spectrum also shows that the molecular nitrogen radiation is asymmetric with respect to the electron beam and is more intense downstream of the beam. Also, since the nitrogen concentration (40 to 400 parts per million) is kept very low in the test gas, the intensity of the molecular nitrogen radiation observed is too high to be attributed to direct excitation by the electron beam. Since the ratio of the excitation cross section for 5016 Å $\left(3^1P - 2^1S\right)$ atomic helium radiation to that for the (0,0) band of the first negative system $\left(B^2\Sigma_u^+ - X^2\Sigma_g^+\right)$ of molecular nitrogen radiation is approximately 2 for electrons with energy of 26 keV, direct excitation cannot account for the strong nitrogen radiation. Both the asymmetry and the strong intensity of the nitrogen radiation indicate the presence of an efficient collision process.

Two possible mechanisms have been suggested (ref. 21) for populating the $B^2\Sigma_u^+$ state of the molecular nitrogen ion:

(1) $He^m + N_2 \rightarrow He + N_2^+ + e$

(2) $He_2^+ + N_2 \rightarrow 2He + N_2^+$

The energy-level diagram in figure 5 shows that mechanisms (1) and (2) represent resonant reactions. In addition, it should be noted that no atomic nitrogen radiation was identified.

Spectrograms taken in regions 3 and 4, downstream from the electron beam, show a large amount of radiation which was identified as molecular helium band spectra. (See fig. 7.) The fact that this radiation occurs downstream from the electron beam with high intensity indicates another very efficient collision process. Niles and Robertson (ref. 8) and Dunn (ref. 21) have attributed this molecular helium radiation to the reactions

$$He^+ + 2He \rightarrow He_2^+ + He$$

$$He_2^+ + e \rightarrow He_2^*$$

$$He_2^* \rightarrow He_2^* \text{ (lower energy)} + h\nu \text{ (band)}$$

The molecular helium radiation was present as far downstream as was observable which corresponds to a duration greater than 500 μsec. (See fig. 3.)

In the region of the electron beam (region 2), the fluorescence should be primarily the result of direct excitation of the gas by the beam. This result is shown in figure 6 where the observed atomic helium radiation is symmetric about the core of the electron beam. Several of the more probable transitions extend several core diameters from the center of the electron beam because of electron scattering and diffusion of resonance radiation.

The radiation which was observed in regions 1, 3, and 4 of figure 3 is shown in figure 7 and is characteristic of the radiation which is present far away from the beam under the test conditions listed in table 1. Generally, the radiation from each of these areas is similar with only the intensity varying. In region 1, the fluorescence from the molecular nitrogen ion predominates with some molecular helium radiation and very weak atomic helium lines. In region 3 the intensity distribution is reversed in that molecular helium is now the primary radiator with nitrogen being secondary and atomic helium again appearing very weakly. Region 4, far downstream is essentially the same as region 1, but now the atomic helium radiation is absent. The spectrum of region 5 of figure 4, which characterizes radiation far upstream, is shown in figure 8. In this region only very weak molecular nitrogen emission is shown. Therefore, the region external to the electron beam can be characterized generally by very weak atomic helium radiation, a predominance of molecular helium radiation just downstream of the beam and a predominance of radiation from the molecular-nitrogen ion far from the beam (both upstream and downstream).

The fluorescence present when shock structure exists in the flow is characterized in the spectrogram of figure 8. Region 6 is characteristic of the radiation present in the strong bow shock. The area covered by the 1.8-cm slit height extends from the inner side of the shock outward. In spectrum A, essentially the only radiation observed is from the molecular nitrogen ion; faint traces of atomic and molecular helium are also present but cannot be seen in the figure. The nitrogen radiation exhibits much more rotational line structure in the shock than elsewhere, and the (0,2) band of the first negative system appears with significant intensity. The atomic helium lines are of constant intensity throughout this region, whereas the molecular helium radiation decreases in intensity toward the center of the shock. With a higher free-stream number density (spectrum B), these trends become clearer and, in addition, the 3889 Å $(3^3P - 2^3S)$ atomic helium

radiation shows a spatial dependence similar to that of nitrogen. The increased nitrogen intensity can be attributed to the increased number density in the shock region resulting in a higher probability of a resonant collision, whereas the increase in band structure of the nitrogen radiation can be attributed to the higher temperature of the shock region.

Region 7 is approximately 1 meter downstream of the electron beam and in the weak wake shock of the wedge. (See fig. 4.) This region is characterized by weak atomic and molecular helium emission and strong molecular nitrogen emission.

The tests with the wedge model indicate that the phenomena observed are basically the same as those in unperturbed flow, except with the wedge model the density and temperature gradients appear as variations in the intensity of molecular helium and nitrogen radiation and thereby the dependence of the emission observed on the number density and temperature of the gas is indicated.

All observations indicate that the region downstream from the electron beam is excited primarily by helium species which are excited by the electron beam and swept downstream. For the upstream region, the fluorescence is attributed to primary beam electrons which are scattered upstream by the tunnel wall (laboratory measurements indicate that 15 percent of a 26-keV electron beam is backscattered from a steel plate). The contribution from secondary electrons emitted at the wall is considered insignificant since they are of low energy and thus their effect is limited to the region near the wall. Hence, the scattered primary electrons can excite the upstream helium. These excited species then can collide with helium atoms and nitrogen molecules to produce the observed fluorescence. Figure 9 shows the effect of the scattered primary electrons. Both photographs were taken under the same test conditions except that an electron collector was present when the second picture was taken. Here the scattering-angle limit imposed by the collector is indicated and the difference in the photographs indicates that scattered electrons are a significant part of the upstream excitation process.

Finally, spectrographic data were taken in a static laboratory test where all test variables, including the experimental setup, were the same as those used in region 2 of figure 3, except that the gas was stationary and tests were made at a static temperature of 300° K. Figure 10 shows the spectrum resulting from this test. The nitrogen radiation observed was comparable in intensity with that observed in the tunnel, but the molecular helium radiation was not detected. The absence of molecular helium radiation indicates that it has an inverse temperature dependence and, therefore, may offer an approach for measuring gas temperature in hypersonic helium flow. However, since for the tunnel tests the nitrogen-impurity concentration could vary from 40 to 400 parts per million and the static tests was performed at a nominal value of 100 parts per million, this suggested temperature dependence should be examined over the entire impurity range of the tunnel.

CONCLUSIONS

The following conclusions can be obtained from the experiments concerning both the use of the electron-beam technique for helium-flow visualization and the characteristics of the radiation observed:

(1) The reaction leading to the fluorescence of the molecular nitrogen ion was found to enhance significantly the use of the electron-beam technique for flow visualization in hypersonic helium-flow studies.

(2) The collision processes leading to the fluorescence of both molecular nitrogen and molecular helium were found to be very efficient at the gas conditions tested (number densities from 6.4×10^{23} to 14.3×10^{23} per m^3, static temperatures of 2.2° to 2.5° K, and a gas composition of 40 to 400 parts per million of molecular nitrogen in helium).

(3) Atomic helium was identified as the primary radiator in the electron beam, whereas molecular helium was the primary radiator near the beam.

(4) Observations of regions in the shock wave and far from the beam have indicated that the molecular nitrogen ion is the primary radiator. In addition, the rotational line structure of the first negative system of nitrogen was observed in the shock and found to reflect the temperature increase through the shock.

(5) The upstream fluorescence has been attributed primarily to high-energy electrons which are scattered from the tunnel wall and excite the helium atoms upstream of the electron beam. These excited species then can collide with helium atoms and nitrogen molecules to produce the observed fluorescence.

(6) The downstream fluorescence has been attributed primarily to collisions of excited helium species (which are produced in the electron beam and carried downstream) with the gas constituents: atomic helium and molecular nitrogen.

(7) A test was conducted with a similar helium and nitrogen gas mixture (100 parts per million of nitrogen) and number density (6×10^{23} per m^3) as those used in the tunnel tests, but with a static temperature of 300° K and stationary gas. This test showed that the molecular helium radiation was not present, and thus a significant inverse temperature dependence was indicated. However, this test does not cover the entire impurity range of the tunnel (40 to 400 parts per million of nitrogen in helium).

Langley Research Center,
National Aeronautics and Space Administration,
Hampton, Va., August 7, 1970.

REFERENCES

1. Williams, Thomas W.; and Benson, James M.: Preliminary Investigation of the Use of Afterglow for Visualizing Low-Density Compressible Flows. NACA TN 1900, 1949.

2. Kunkel, W. B.; and Hurlbut, F. C.: Luminescent Gas Flow Visualization in a Low-Density Supersonic Wind Tunnel. WADC Tech. Rep. 57-441, DDC No. AD 151 007, U.S. Air Force, Sept. 1957.

3. Grün, A. E.; Schopper, E.; and Schumacher, B.: Electron Shadowgraphs and Afterglow Pictures of Gas Jets at Low Densities. J. Appl. Phys., vol. 24, no. 12, Dec. 1953, pp. 1527-1528.

4. Sebacher, Daniel I.: Primary and Afterglow Emission From Low-Temperature Gaseous Nitrogen Excited by Fast Electrons. J. Chem. Phys., vol. 44, no. 11, June 1, 1966, pp. 4131-4136.

5. Maguire, Bernadette L.; Muntz, E. Phillip; and Mallin, John R.: Visualization Technique for Low-Density Flow Fields. IEEE Trans. Aerosp. Electron. Syst., vol. 3, no. 2, Mar. 1967, pp. 321-326.

6. Rothe, Dietmar E.: Flow Visualization Using a Traversing Electron Beam. AIAA J., vol. 3, no. 10, Oct. 1965, pp. 1945-1946.

7. Merton, T. R.; and Pilley, J. G.: Spectrum of Nitrogen. Proc. Roy. Soc. (London), ser. A, vol. 107, Mar. 2, 1925, pp. 411-422.

8. Niles, Franklin E.; and Robertson, W. W.: Spectral Emission of the Helium Afterglow. J. Chem. Phys., vol. 40, no. 10, May 15, 1964, pp. 2909-2914.

9. Collins, C. B.; and Robertson, W. W.: Spectra Excited in a Helium Afterglow. J. Chem. Phys., vol. 40, no. 3, Feb. 1, 1964, pp. 701-712.

10. Robertson, W. W.: Application of the Franck-Condon Principle to Molecular Excitation by Collision With Excited Atoms and Molecules. J. Chem. Phys., vol. 44, no. 6, Mar. 15, 1966, pp. 2456-2461.

11. Fehsenfeld, F. C.; Schmeltekopf, A. L.; Goldan, P. D.; Schiff, H. I.; and Ferguson, E. E.: Thermal Energy Ion-Neutral Reaction Rates. I. Some Reactions of Helium Ions. J. Chem. Phys., vol. 44, no. 11, June 1, 1966, pp. 4087-4094.

12. Goldan, P. D.; Schmeltekopf, A. L.; Fehsenfeld, F. C.; Schiff, H. I.; and Ferguson, E. E.: Thermal Energy Ion-Neutral Reaction Rates. II. Some Reactions of Ionospheric Interest. J. Chem. Phys., vol. 44, no. 11, June 1, 1966, pp. 4095-4103.

13. Ferguson, E. E.; Fehsenfeld, F. C.; and Schmeltekopf, A. L.: Dissociative Recombination in Helium Afterglows. Phys. Rev., Second ser., vol. 138, no. 2A, Apr. 19, 1965, pp. A381-A385.

14. Phelps, Arthur V.; and Brown, Sanborn C.: Positive Ions In the Afterglow of a Low Pressure Helium Discharge. Phys. Rev., Second ser., vol. 86, no. 1, Apr. 1, 1952, pp. 102-105.

15. Schmeltekopf, A. L.; Ferguson, E. E.; and Fehsenfeld, F. C.: Afterglow Studies of the Reactions He^+, $He(2^3S)$, and O^+ With Vibrationally Excited N_2. J. Chem. Phys., vol. 48, no. 7, Apr. 1, 1968, pp. 2966-2973.

16. Schmeltekopf, Arthur L., Jr.; and Broida, H. P.: Short-Duration Visible Afterglow in Helium. J. Chem. Phys., vol. 39, no. 5, Sept. 1, 1963, pp. 1261-1268.

17. Warneck, Peter: Studies of Ion-Neutral Reactions by a Photoionization Mass-Spectrometer Technique. IV. Reactions of He^+ With N_2 and O_2. J. Chem. Phys., vol. 47, no. 10, Nov. 15, 1967, pp. 4279-4281.

18. Weinstein, Leonard M.; Wagner, Richard D., Jr.; and Ocheltree, Stewart L.: Electron Beam Flow Visualization in Hypersonic Helium Flow. AIAA J., vol. 6, no. 8, Aug. 1968, pp. 1623-1625.

19. Exton, R. J.; and Houghton, W. M.: Portable Survey Spectrograph. Rev. Sci. Instrum., vol. 35, no. 10, Oct. 1964, p. 1370.

20. Schaefer, William T., Jr.: Characteristics of Major Active Wind Tunnels at the Langley Research Center. NASA TM X-1130, 1965.

21. Dunn, Jerry L.: Spectral Analysis of Mechanisms and Kinetics of Thermal Energy Reactions of Long-Lived Energetic Helium Species With Simple Molecules. Ph. D. Thesis, Univ. of California, 1966.

TABLE 1.- TEST CONDITIONS

[Velocity, 1.8 km/sec; stagnation temperature, 300° K; exposure time, 37 sec]

Region	Mach number	Stagnation pressure, MN/m^2	Static temperature, ^{o}K	Static number density, per m^3	Spectrograph	Slit width, μm	ASA film-speed rating
1	19.1	3.4	2.5	6.4×10^{23}	Survey	≈ 100	10 000
2	20.3	6.9	2.2	14.3	High resolution	100	3 000
3	19.1	3.4	2.5	6.4	High resolution	300	3 000
4	19.1	3.4	2.5	6.4	Survey	≈ 100	10 000
5	19.1	3.4	2.5	6.4	High resolution	100	3 000
6 A	19.1	3.4	2.5	6.4	High resolution	100	3 000
6 B	20.3	6.9	2.2	14.3	High resolution	300	3 000
7	19.1	3.4	2.5	6.4	Survey	≈ 500	10 000

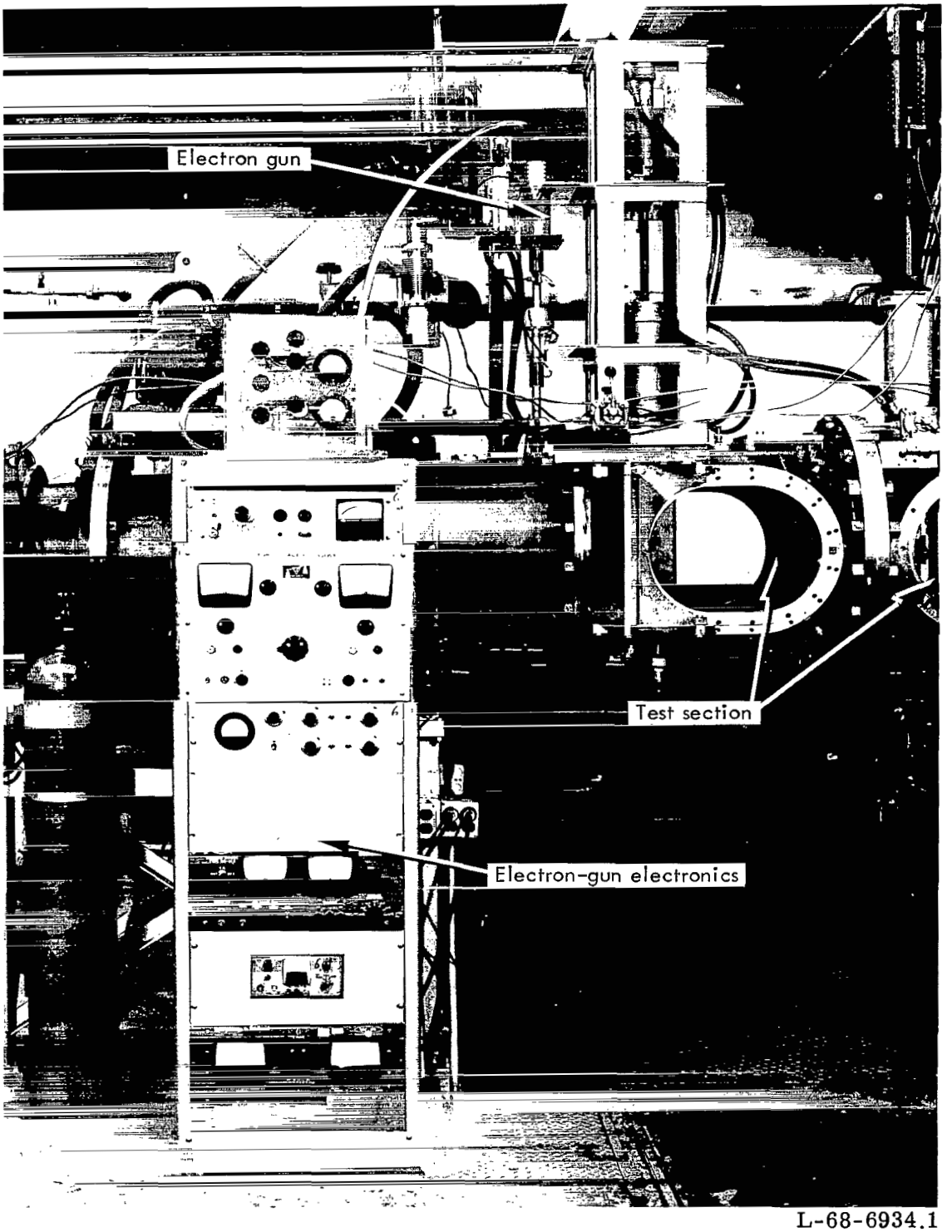

L-68-6934.1

Figure 1.- Electron gun and helium-tunnel test section.

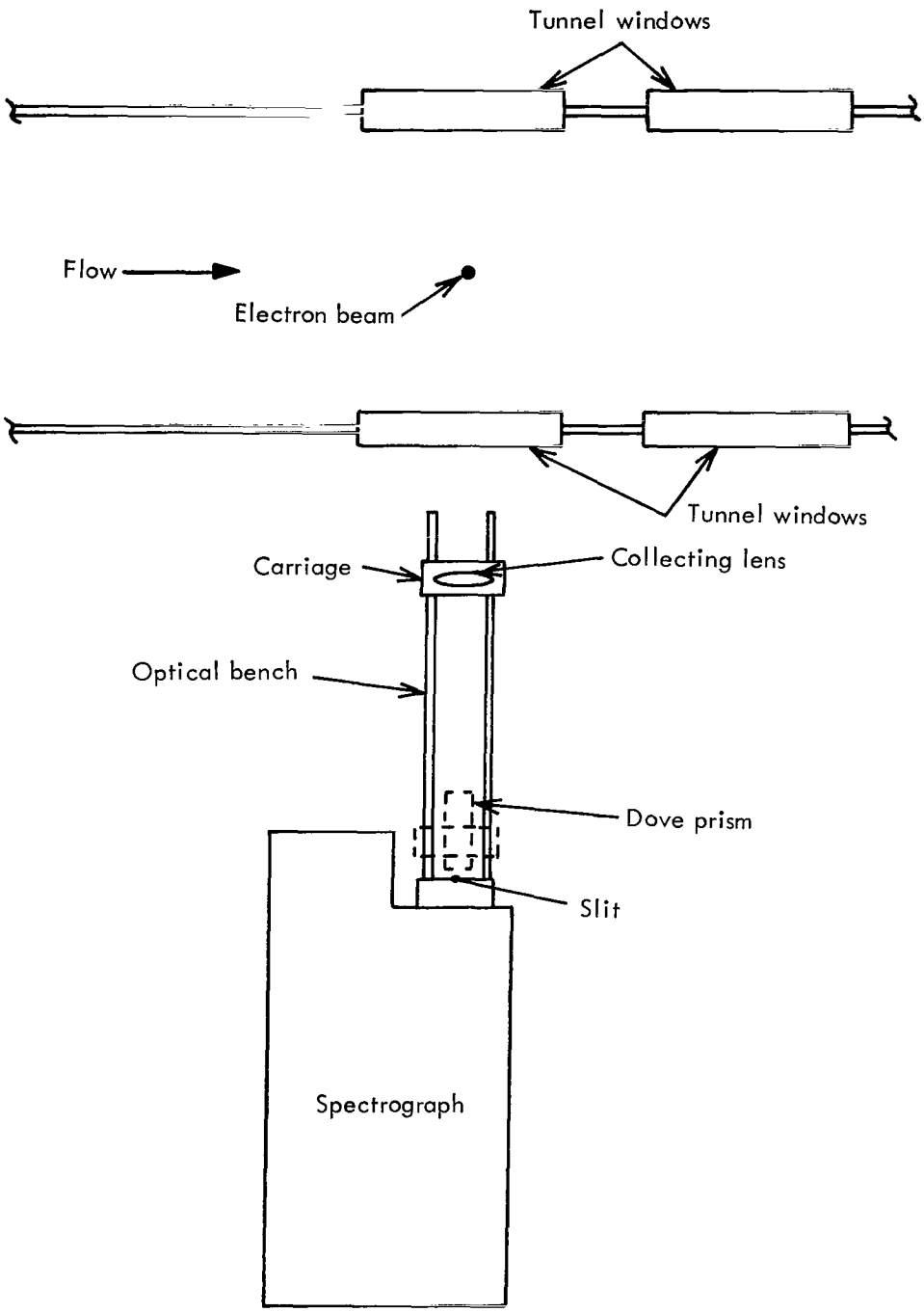

Figure 2.- Optical arrangement.

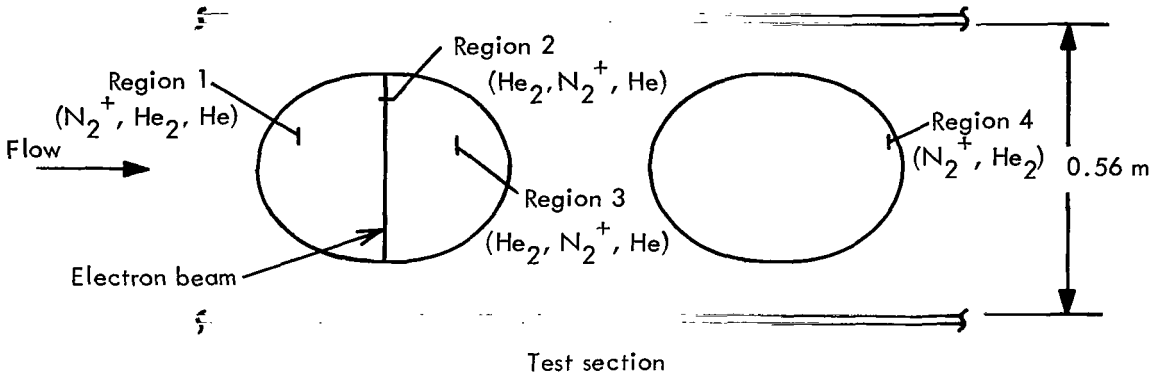

Figure 3.- Scale drawing of regions representative of fluorescence for undisturbed flow with the three primary radiators listed in order of decreasing intensity for each region. Velocity, 1.8 km/sec.

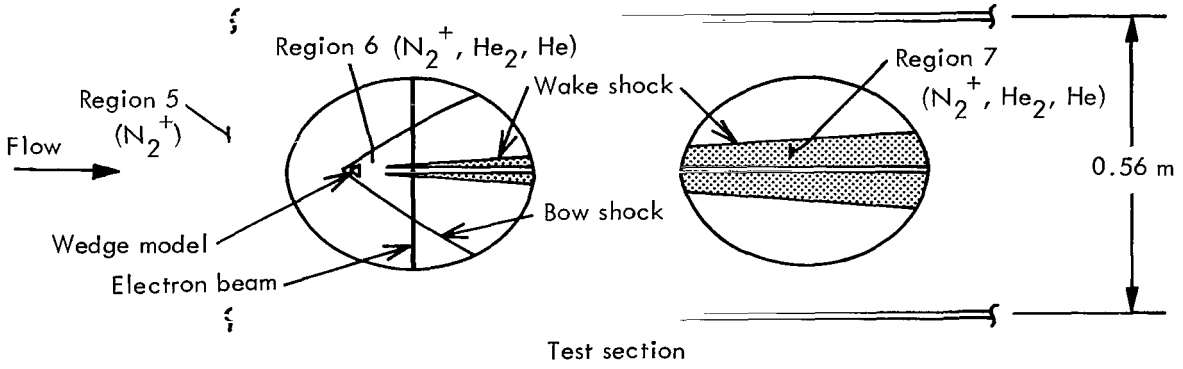

Figure 4.- Scale drawing of regions representative of fluorescence with shock structure with the three primary radiators listed in order of decreasing intensity for each region. Velocity, 1.8 km/sec.

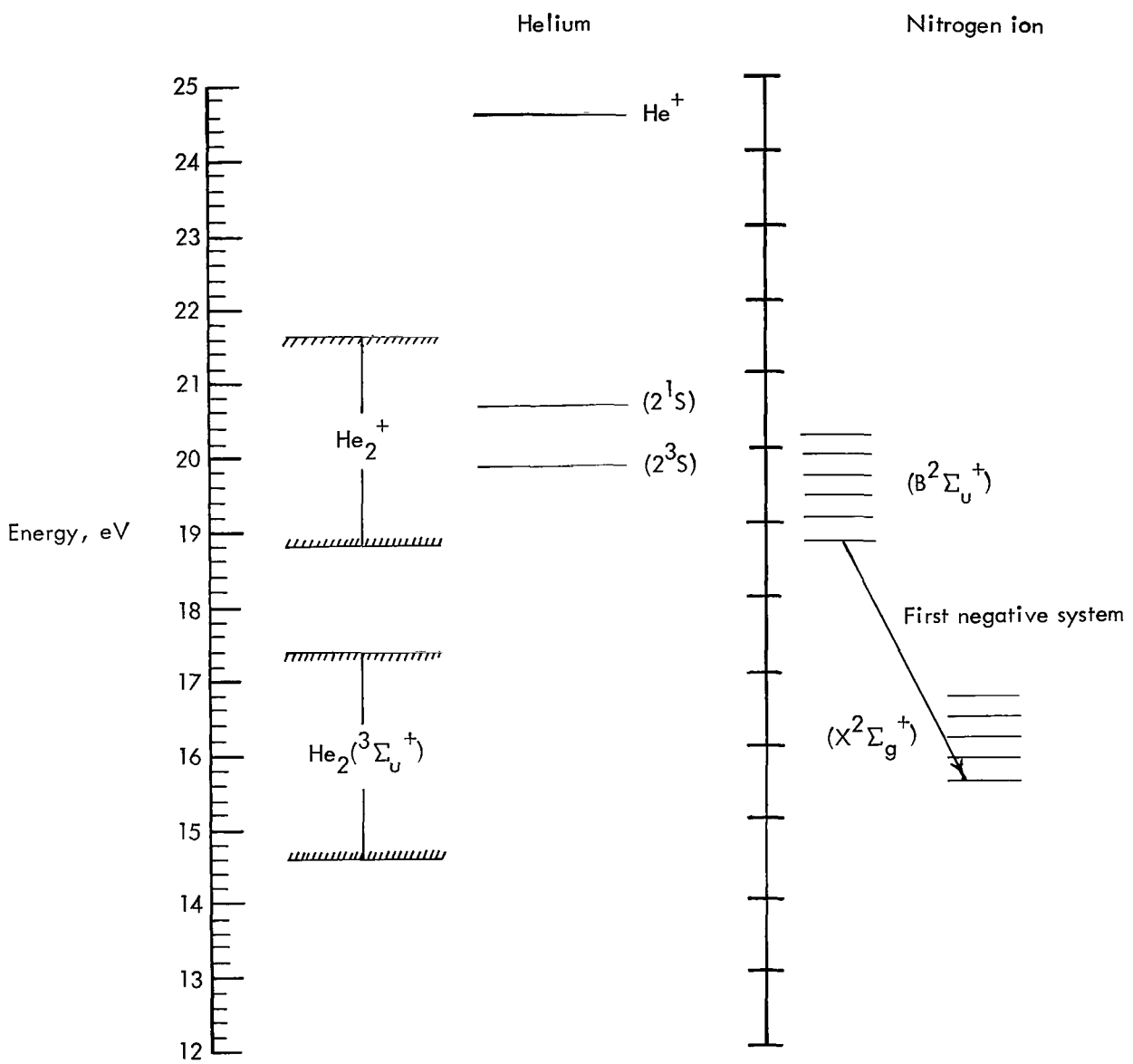

Figure 5.- Energy-level diagrams for the active helium species and the molecular nitrogen ion.

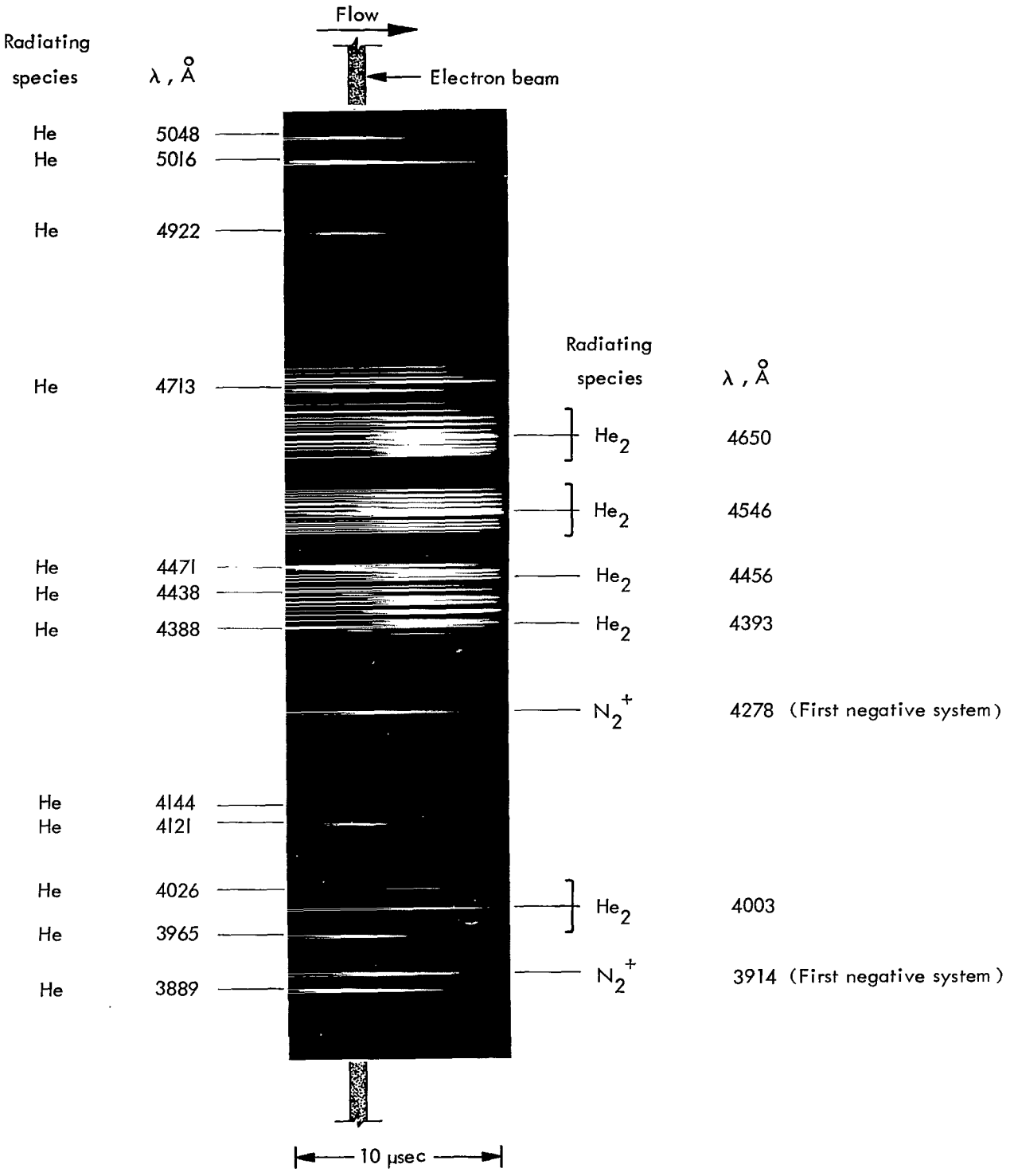

Figure 6.- Spectrum of fluorescence in and near electron beam. Velocity, 1.8 km/sec.

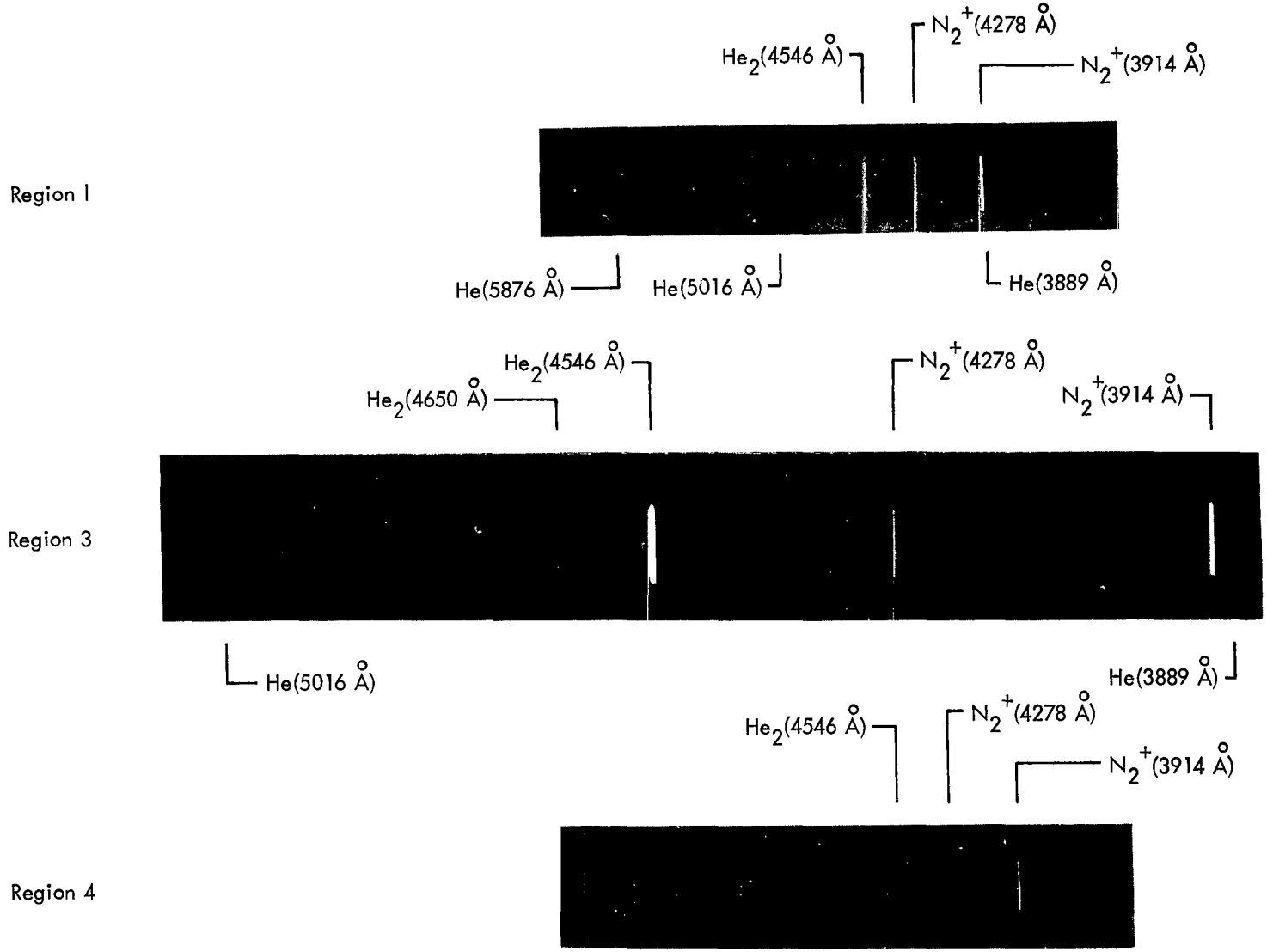

Figure 7.- Spectra of the unperturbed flow. (Wavelengths are given parenthetically.)

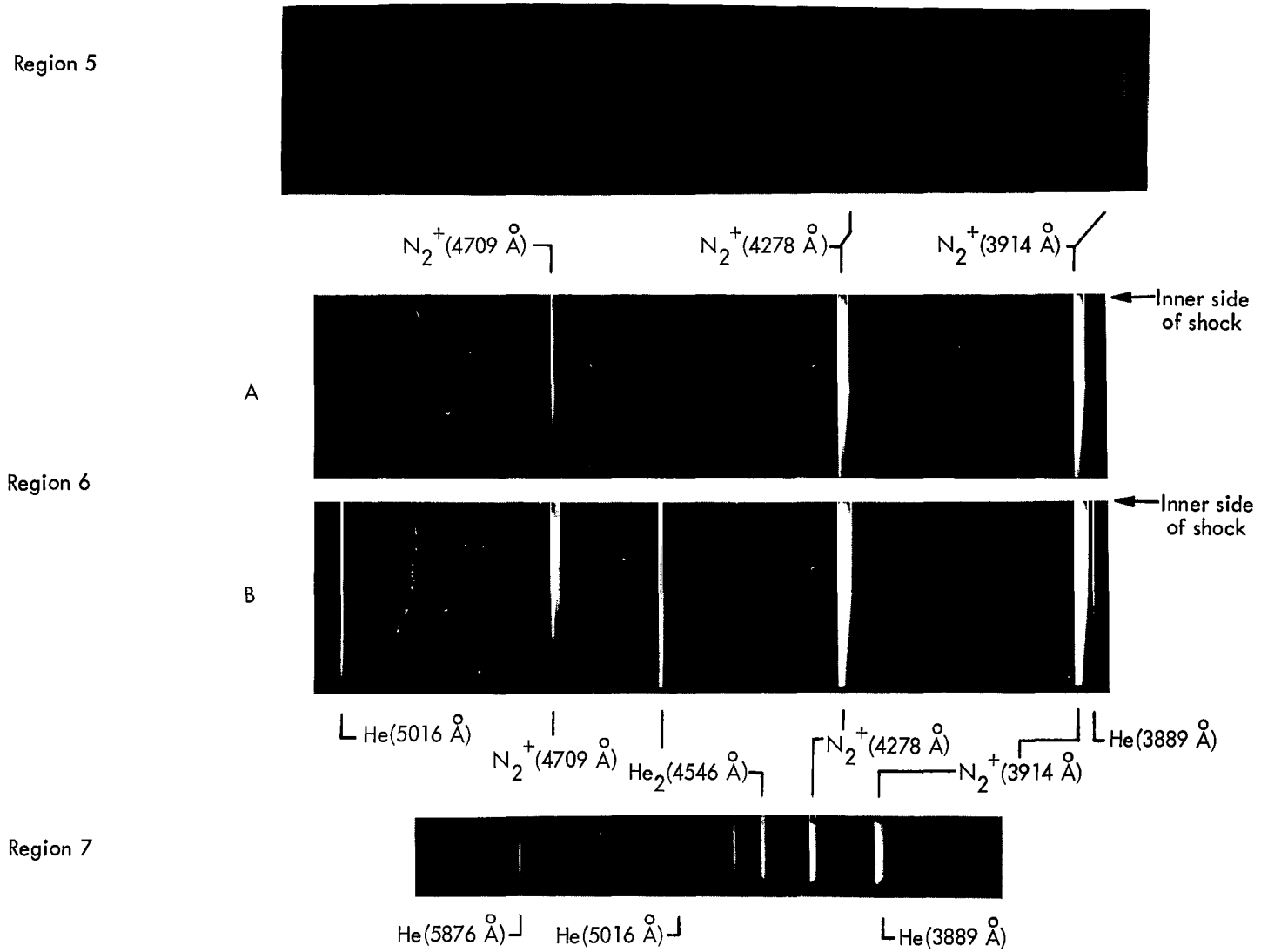

Figure 8.- Spectra of flow with shock structure. (Wavelengths are given parenthetically.)

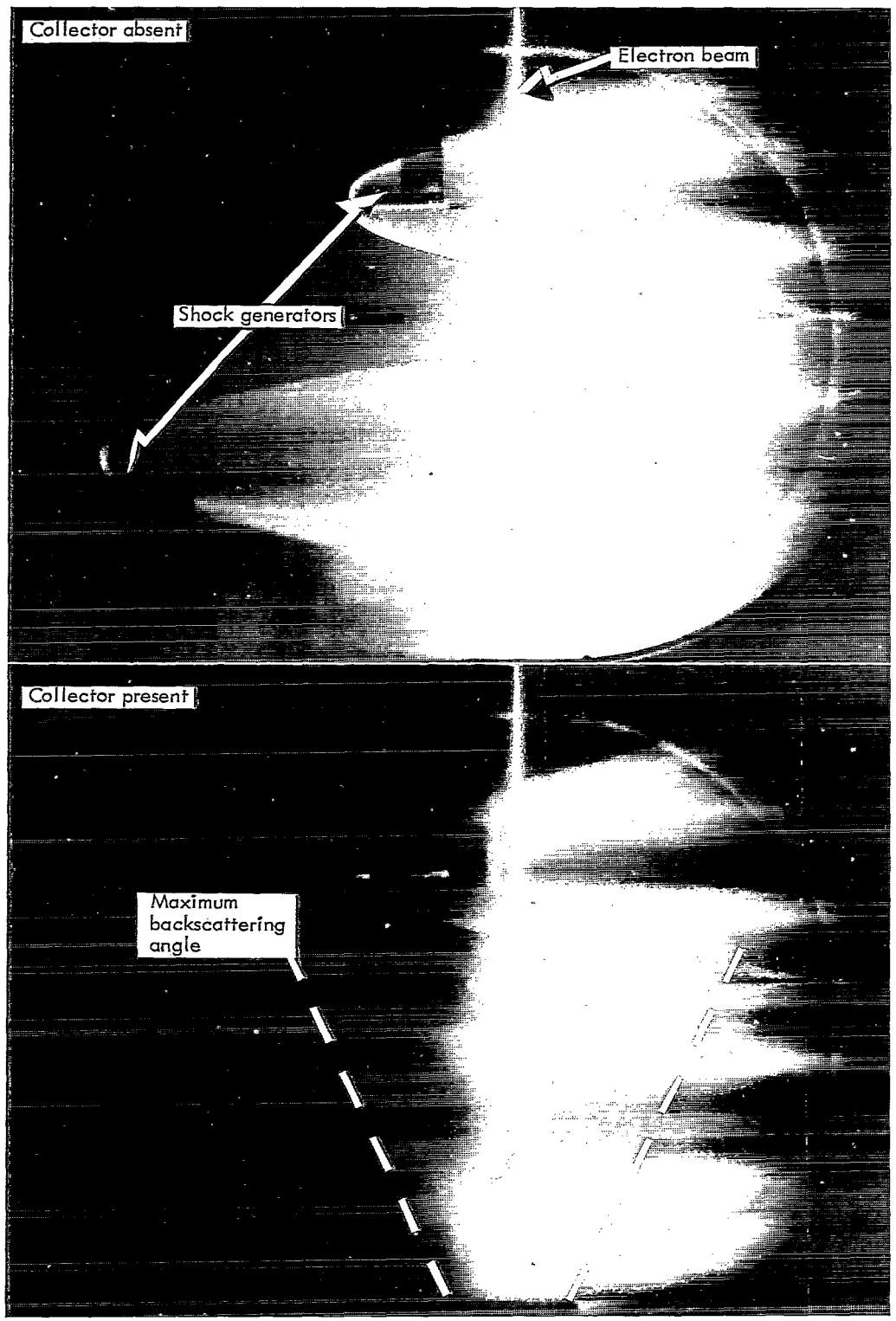

Figure 9.- Effect of reflected electrons.

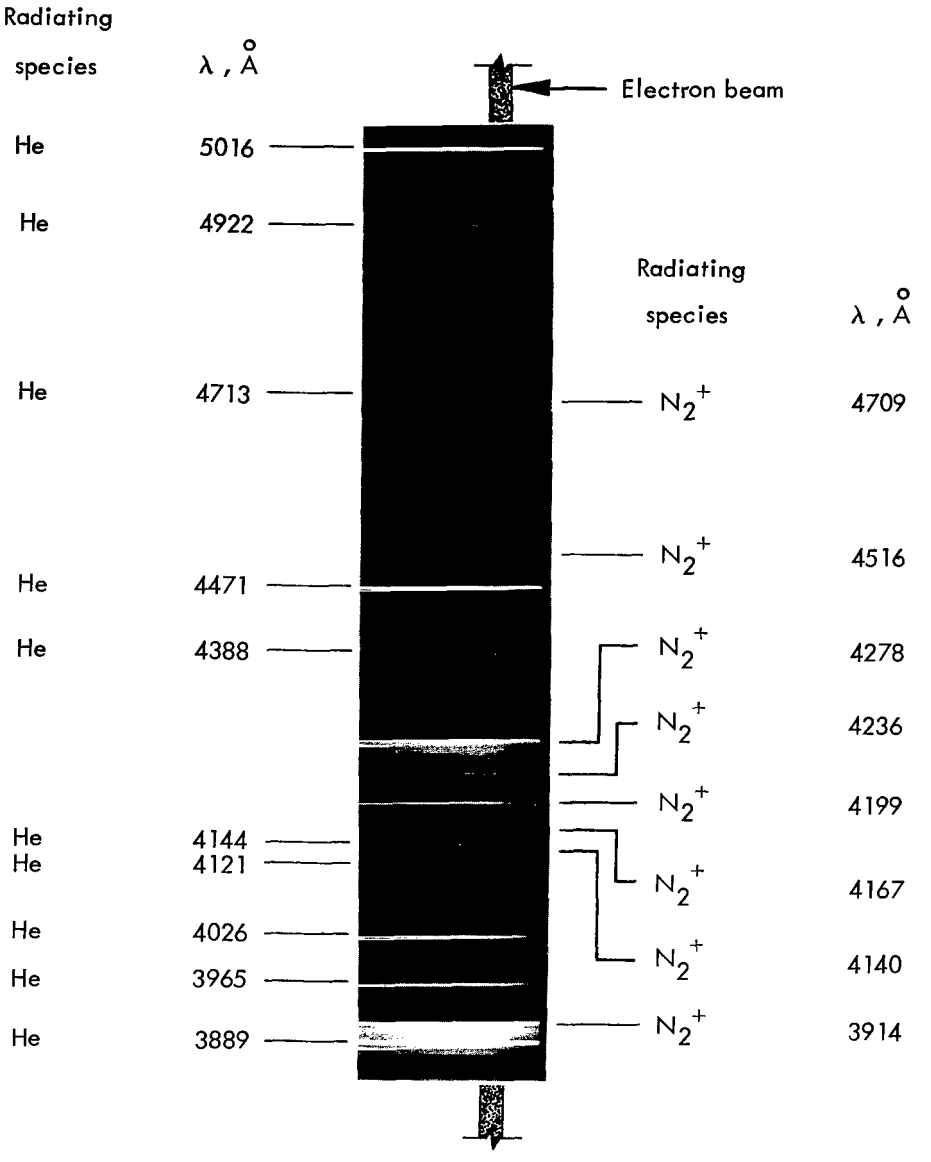

Figure 10.- Spectrum of a static He and N_2 mixture at 300° K.

"The aeronautical and space activities of the United States shall be conducted so as to contribute . . . to the expansion of human knowledge of phenomena in the atmosphere and space. The Administration shall provide for the widest practicable and appropriate dissemination of information concerning its activities and the results thereof."

—NATIONAL AERONAUTICS AND SPACE ACT OF 1958

NASA SCIENTIFIC AND TECHNICAL PUBLICATIONS

TECHNICAL REPORTS: Scientific and technical information considered important, complete, and a lasting contribution to existing knowledge.

TECHNICAL NOTES: Information less broad in scope but nevertheless of importance as a contribution to existing knowledge.

TECHNICAL MEMORANDUMS: Information receiving limited distribution because of preliminary data, security classification, or other reasons.

CONTRACTOR REPORTS: Scientific and technical information generated under a NASA contract or grant and considered an important contribution to existing knowledge.

TECHNICAL TRANSLATIONS: Information published in a foreign language considered to merit NASA distribution in English.

SPECIAL PUBLICATIONS: Information derived from or of value to NASA activities. Publications include conference proceedings, monographs, data compilations, handbooks, sourcebooks, and special bibliographies.

TECHNOLOGY UTILIZATION PUBLICATIONS: Information on technology used by NASA that may be of particular interest in commercial and other non-aerospace applications. Publications include Tech Briefs, Technology Utilization Reports and Notes, and Technology Surveys.

Details on the availability of these publications may be obtained from:

SCIENTIFIC AND TECHNICAL INFORMATION DIVISION

NATIONAL AERONAUTICS AND SPACE ADMINISTRATION

Washington, D.C. 20546